

Slot-Level Robotic Placement via Visual Imitation from Single Human Video

Dandan Shan^{1,2*} Kaichun Mo^{1†} Wei Yang¹
 Yu-Wei Chao¹ David Fouhey³ Dieter Fox^{1,4} Arsalan Mousavian¹
¹ NVIDIA Research ² Univ. of Michigan ³ NYU ⁴ Univ. of Washington
<https://ddshan.github.io/slerp>

Abstract

The majority of modern robot learning methods focus on learning a set of pre-defined tasks with limited or no generalization to new tasks. Extending the robot skillset to novel tasks involves gathering an extensive amount of training data for additional tasks. In this paper, we address the problem of teaching new tasks to robots using human demonstration videos for repetitive tasks (e.g., packing). This task requires understanding the human video to identify which object is being manipulated (the pick object) and where it is being placed (the placement slot). In addition, it needs to re-identify the pick object and the placement slots during inference along with the relative poses to enable robot execution of the task. To tackle this, we propose SLeRP, a modular system that leverages several advanced visual foundation models and a novel slot-level placement detector Slot-Net, eliminating the need for expensive video demonstrations for training. We evaluate our system using a new benchmark of real-world videos. The evaluation results show that SLeRP outperforms several baselines and can be deployed on a real robot.

1. Introduction

Humans demonstrate exceptional skill in performing fine-grained manipulation tasks with high precision in their daily lives. From arranging eggs in an egg carton to sorting utensils in an organizer, we excel at tasks that require identifying and reasoning about which objects to pick up and how to place them into confined slots. Cognitive and motor development theories suggest that we develop such skills at a young age, based on early experiences like playing with shape sorter toys [48]. However, current robotic and automated systems are not yet as adept as humans at perceiving and performing these fine-grained manipulation tasks.

Slot-level manipulation is crucial in various industrial, logistics, and domestic contexts. For example, in industrial settings, machine tending [56] requires placing components

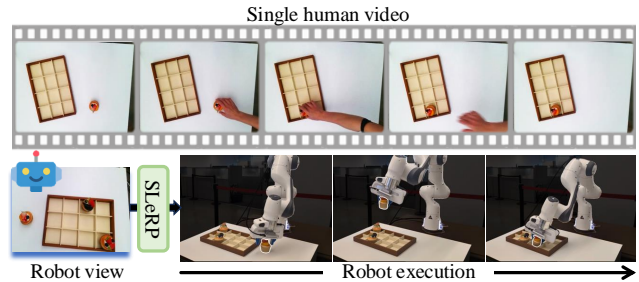


Figure 1. We introduce the novel problem of imitating slot-level robotic placement from a single human video. Given a human demonstration video showing an object being placed in a slot, and a new robot-view image captured by the robot wrist camera (may feature varied camera and object poses, changed scenes), SLeRP is able to find the corresponding object and similar slots in the robot view, and provide the 6-DoF transformation matrix for each detected slot to guide the robot in placing the object accurately.

precisely into machine slots for assembly or processing. In logistics, sorting and packaging tasks, such as organizing parcels in a warehouse or placing products into shipping containers, demand efficient and precise placement to optimize space and minimize damage. In domestic environments, future home assistant robots will need to perform slot-level manipulation tasks such as organizing items in cabinets, placing dishes in a dishwasher, and even preparing meals by accurately arranging ingredients in a pan.

The task of programming robots to perform slot-level placement remains arduous. Traditional methods [19, 66] often require manual programming with domain expertise and assume that the object models and slot locations are known beforehand. Learning-based approaches [8, 29] show promise in alleviating the burden of programming; however, collecting robot data through tele-operation remains tedious and inefficient and can be particularly brittle for high-precision tasks due to embodiment gaps. Learning from human demonstration videos has recently emerged as a promising approach due to its ease, speed of collection, and potential to capture slot-level details. However, previous research [3, 6, 25, 75, 84] has generally been limited to

* Work done during internship at Nvidia. † Primary mentor.

coarser object-level tasks and often requires large amounts of training data to learn how to parse human demonstrations and translate them into robot policies.

In this paper, we study the novel problem of recognizing slot-level object placement from a *single* human video, and estimating 6-DoF transformations for robot imitation. As shown in Fig. 1, the task takes two visual inputs: (1) a single human RGB-D video in which a person demonstrates picking up an object (*e.g.*, a muffin) and precisely placing it into a slot within a placement object (*e.g.*, a tray), and (2) a single RGB-D image captured from the robot’s wrist camera, representing the new setup for the robot to operate in with possible varying camera and object poses compared to the human video. The outputs aim to detect the object and all empty slots in the robot’s view similar to the placement slot in the human video, as well as compute the 6-DoF object transformations necessary for the robot to transfer the object from its initial position to each of the slots.

We propose a novel modular approach called SLeRP (*i.e.*, **Slot-Level Robotic Placement**), to tackle the problem. As shown in Fig. 2, SLeRP starts by analyzing the input human demonstration video, tracking the manipulated object across the video frames and identifying the placement slot. Next, within the robot’s view, SLeRP re-identifies both the object and the slot by correlating the human-view images with the robot-view images. By lifting the observations in 3D using the depth sensing and camera parameters, SLeRP calculates a 6-DoF transformation matrix for the robot to transfer the object from its initial location to the desired slot in the robot’s view. If multiple slots are present, SLeRP detects all slots that are similar to the one in the human video and computes the object transformations for all of them. Finally, the computed 6-DoF object transformations are sent to the downstream robot planning and control pipeline for robot pick-and-place execution.

A key component of SLeRP is the detection of placement slots. Currently, no existing method is specifically designed for this task, and simple image differencing or change detection [17] does not effectively solve the problem. Therefore, we propose a new slot-level placement detector, Slot-Net, that takes two image frames from a human demonstration video—one before and one after placement—and outputs a 2D mask outlining the placement slot on the images. Unlike common vision tasks, collecting a sizable training dataset for slot-level placement detection is challenging. To address this challenge, we introduce a generative AI-based data creation pipeline that expands the training set by bootstrapping from a small set of images.

For evaluation, we introduce a new dataset comprising 288 real-world videos targeted at studying this novel problem. We compare our method against several baseline approaches, including ORION [84], a state-of-the-art method for object-level pick-and-place from a sin-

gle human video; CLIPort [60], an end-to-end imitation-learning-based language-conditioned policy for tabletop tasks; adapted versions of both for the novel slot-level task; and a custom baseline leveraging cutting-edge vision-language models like GPT-4o [24]. Our results demonstrate that SLeRP outperforms baselines in accurately predicting placement slots and computing 6-DoF transformations across diverse real-world tasks. Our ablation studies further validate several key components and design choices in our system. Finally, we conduct real-robot experiments that successfully apply the system in real world scenarios.

In summary, the core contributions of this paper are:

- Studying the novel task of slot-level object placement by learning from a single human demonstration video;
- Designing the modular approach SLeRP and the slot-level placement detector Slot-Net to tackle this problem;
- Introducing a new benchmark and several baseline methods to systematically evaluate system performance;
- Demonstrating that SLeRP achieves strong performance in real-world and real-robot evaluations.

2. Related Work

Object Placement in Robotics. Identifying where and how to place an object after picking it up is a crucial step in robotic pick-and-place tasks [36]. Early works [5, 21, 22] analytically search for flat features on the object and the placement surface. Modern learning-based methods estimate placement locations and poses using learned features, focusing mainly on flat surfaces [45], such as tabletop [12, 42, 81] and furniture shelves [43]. Researchers have also explored tabletop object placement under spatial and semantic constraints given other objects [34, 41, 51].

In the more challenging case of placing an object on another non-flat object, prior work [15, 27, 49, 58, 61, 62, 65, 72, 84] has explored tasks like putting one spoon in a cup or hanging a mug on a rack. Our work extends these studies by focusing on placing objects into all empty, fine-grained, tight-fitting slots (*e.g.*, all egg slots in a carton), a task that demands greater precision in recognition and prediction, as well as handling multiple placement locations. Additionally, unlike previous work [23, 60, 74, 82, 83] that addresses a 2D planar setting and requires task-specific training from a few robot demonstrations, our approach tackles this problem in 3D, learning from a single human demonstration to enable one-shot generalization to novel tasks.

Imitation Learning from Human Videos. Human videos serve as a natural, information-rich, and easily accessible source of data for learning robotic manipulation. Previous work has explored diverse methods to extract, represent, and apply knowledge from human videos to support robot manipulation learning. These approaches include pre-training latent visual representations [14, 38, 44, 57], inferring action trajectories or plans [3, 31, 46, 70, 78], learn-

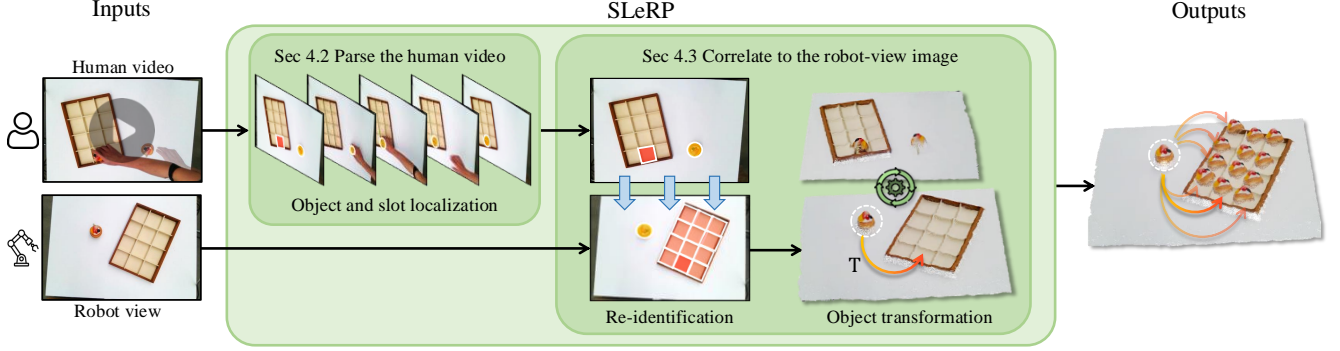


Figure 2. **Method Overview.** The system begins by analyzing the input human video, tracking the object (highlighted in yellow) throughout the sequence and identifying the placement slot (highlighted in red). Next, we re-identify the object and the slot in the robot’s view by correlating the human-view and robot-view images. Using depth images, we reconstruct the observations in 3D and compute a single 6-DoF object transformation T in the robot’s view, enabling the robot to transfer the object into the slot. If more than one slot is present, we detect all applicable slots and compute one 6-DoF object transformation for each slot. Finally, such 6-DoF object transformations are sent to the downstream robot planning and control pipeline for real robot pick-and-place execution.

ing value or reward functions [9, 37], reconstructing human hand or hand-object interaction [40, 50, 53, 59, 63], parsing interaction goals and affordance [4, 28, 35, 77], learning point tracks for human-to-robot transfer [7, 73, 75, 76, 80], etc. While the primary goals of these works are typically learning robot trajectories or manipulation policies, our work explores a novel perspective by recognizing fine-grained placement slots as visual imitation targets.

Additionally, we tackle robot imitation learning from a single human video. Previous work has investigated one-shot [13, 25, 26, 39, 79] and even zero-shot learning from human videos [6]; however, these approaches often require extensive human video datasets, sometimes paired with robot videos, to span multiple tasks during training. In contrast, our approach leverages existing visual foundation models, eliminating the need for large-scale training videos. A notably similar work ORION [84] relies on text to recognize task-relevant objects and primarily focuses on object-level pick-and-place. In contrast, our method exclusively extracts information from a single human video to perform more fine-grained slot-level placement tasks.

3. Problem Formulation

We formulate the novel problem of recognizing slot-level object placement from a single human video, and estimating 6-DoF transformations for downstream robot imitation.

Inputs. The task takes the following inputs:

- a single RGB-D human demonstration video with n frames, denoted as $\mathcal{H} = \{\mathbf{H}_1, \mathbf{H}_2, \dots, \mathbf{H}_n\}$, recording a person picking up an object O from the scene and placing it in a slot S within a placement object;
- a single RGB-D robot-view image \mathbf{R} that captures the robot’s observation, often taken from the robot wrist camera and possibly with different camera and object poses, or scene layouts.

Outputs. The task outputs, in the robot’s view, are:

- an object mask \mathbf{M}_R^O over the robot image \mathbf{R} that segments the object O to pick;
- a list of slot masks $\{\mathbf{M}_R^{S_0}, \mathbf{M}_R^{S_1}, \dots, \mathbf{M}_R^{S_k}\}$ over the robot image \mathbf{R} that marks all empty slots on the placement object similar to the demonstrated placement slot in the human video \mathcal{H} ;
- a list of 3D 6-Degree-of-Freedom (DoF) object transformation matrices $\{\mathbf{T}_0, \mathbf{T}_1, \dots, \mathbf{T}_k \mid \mathbf{T}_i \in SE(3)\}$ in the robot’s coordinate frame, for the robot to transfer the object O from its initial position to all the detected slots.

Passing the detected object and slot masks, as well as the calculated 6-DoF object transformation matrices, downstream robot pick-and-place pipeline is able to execute slot-level object placement as shown in Fig. 1.

4. Method

In this section, we present the technical designs of SLeRP. We begin with an overview (Sec. 4.1) and then dive into more details in parsing the input human video (Sec. 4.2) and correlating to the robot’s view image (Sec. 4.3).

4.1. System Overview

Taking as inputs a human demonstration video \mathcal{H} and a robot-view image \mathbf{R} , our method SLeRP (Fig. 2) starts with parsing the input human video (Sec. 4.2) by tracking the object O throughout the video frames and identifying the placement slot S . After this process, we obtain an object mask $\mathbf{M}_{H_1}^O$ and a slot mask $\mathbf{M}_{H_1}^S$ over the first frame of the human video \mathbf{H}_1 . Next, by leveraging this information, SLeRP correlates the human-view and robot-view images (Sec. 4.3), and re-identify the object mask \mathbf{M}_R^O and the slot mask $\mathbf{M}_R^{S_0}$ in the robot-view image \mathbf{R} , as observed in the first human frame. If multiple similar slots are present, the system detects other empty slots $\{\mathbf{M}_R^{S_1}, \dots, \mathbf{M}_R^{S_k}\}$ as well. Then, the system lifts the human and robot observa-

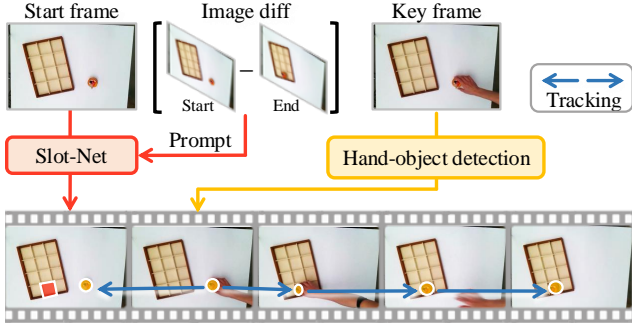


Figure 3. **Parse Human Video.** Given the input human video (bottom), we run state-of-the-art hand-object detector (yellow) and tracker (blue) to obtain the pick object mask (yellow) and train a novel network Slot-Net (red) to identify the slot mask (red).

tions in 3D using the depth sensing and camera intrinsics, and computes a single 6-DoF object transformation matrix $\mathbf{T}_i \in SE(3)$ for each detected slot $\mathbf{M}_{R_i}^{S_i}$.

4.2. Parsing the Human Demonstration Video

The input human video precisely demonstrates what is the pick object O and where is the placement slot S . As shown in Fig. 3, our method utilizes powerful hand-object detection and tracking systems to identify the object mask $\mathbf{M}_{H_1}^O$ and proposes a novel network Slot-Net for estimating the slot mask $\mathbf{M}_{H_1}^S$ over the first frame of the human video.

Object detection and tracking. We use a hand-object detector [10] to detect frame-wise hands and in-contact objects, enabling us to locate the pick object O in the human video. As the detector operates on a per-frame basis, there may be temporally inconsistent predictions. To refine the detection results, we apply MASA’s matching algorithm [33] to generate smooth trajectories for the hand and pick object across the hand-object contact frames. We then identify a confident key frame, when the hand and object first interacts, and use SAM2 [54] to track through the video, producing per-frame object segmentation $\mathbf{M}_{H_i}^O$.

Placement slot detection (Slot-Net). Since no prior work has studied the problem of detecting the placement slot given a human pick-and-place video, we propose our own novel network Slot-Net for this purpose. We leverage the SAM architecture [30] as the backbone given its powerful capability in segmentation. Slot-Net takes the starting frame \mathbf{H}_1 of the pick-place video as the input, together with the absolute image difference in gray-scale between the starting and end frame $|\mathbf{H}_1 - \mathbf{H}_n|$ as the visual prompt, and is tasked to output a slot segment in the starting human frame image $\mathbf{M}_{H_1}^S$. We leverage SAM’s large-scale pretraining by preserving most of its designs (*e.g.*, the image encoder, the mask decoder) and we use the same image encoder as the prompt embedder to process image difference prompt. Since we find that the SAM pretraining does not directly work on such customized new task, finetuning over such

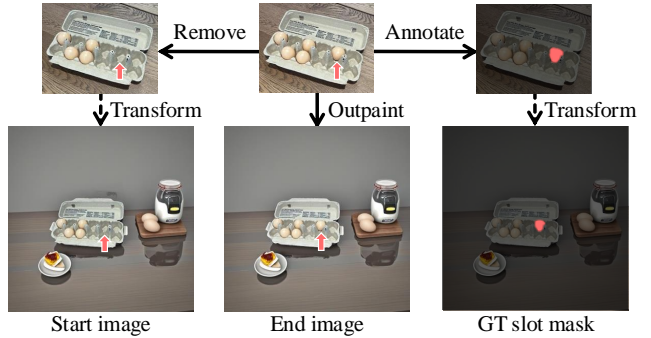


Figure 4. **Slot-Net Data Generation.** Given an object-centric image (top middle), we inpaint to remove an object and reveal its slot (top left) and manually annotate the slot mask (top right). We then outpaint these images with a scene background (bottom) to create a starting and end image pair with a ground-truth slot mask.

slot-level placement data is necessary.

Slot-Net data generation. Training our SAM-based SLeRP requires a lot of data, yet collecting fine-grained slot-level placement data in the real world is expensive. However, recent generative models have demonstrated great capabilities in generating realistic images [52], excelling at tasks such as object removal and image outpainting. We therefore propose a semi-automatic synthetic data generation pipeline (Fig. 4). Given a collected object-centric image of a placement object with many slots, we utilize a state-of-the-art object removal model (SDXL [69] and Cleanup.pictures [11]) to remove one pick object from one slot and manually annotate the slot mask for the removed object using TORAS [64]. Then, we employ a powerful image outpainting generative model (Hugging Face Outpainting script [1]) to expand the image canvas, generating 100 images in diverse backgrounds, prompted with Llama [68] generated text prompts, for each object-centric image.

In this manner, we obtain a large number of annotated starting and end image pairs to train SLeRP. We crowd-sourced and collected 2,138 object-centric images of items with slots, spanning 67 object categories, by capturing them in everyday environments. We applied 100 augmentations for each slot on the object-centric image, resulting in 156K images for training, with the rest left for testing and validation. See supplementary for more details.

4.3. Correlating to the Robot-view Image

After we obtain the pick object mask $\mathbf{M}_{H_1}^O$ and the slot mask $\mathbf{M}_{H_1}^S$ from the human video, the next step is to correlate this information to the robot’s view \mathbf{R} . As shown in Fig. 5, SLeRP first re-identifies the object mask $\mathbf{M}_{\mathbf{R}}^O$ and a list of empty slot masks $\{\mathbf{M}_{\mathbf{R}}^{S_0}, \mathbf{M}_{\mathbf{R}}^{S_1}, \dots, \mathbf{M}_{\mathbf{R}}^{S_k}\}$ similar to the human demonstrated placement slot. Then, 2D keypoint matching and 3D lifting enable the calculation of a single 6-DoF object transformation matrix $\mathbf{T}_i \in SE(3)$ for each detected slot $\mathbf{M}_{\mathbf{R}}^{S_i}$ for downstream robotic pick-and-place.

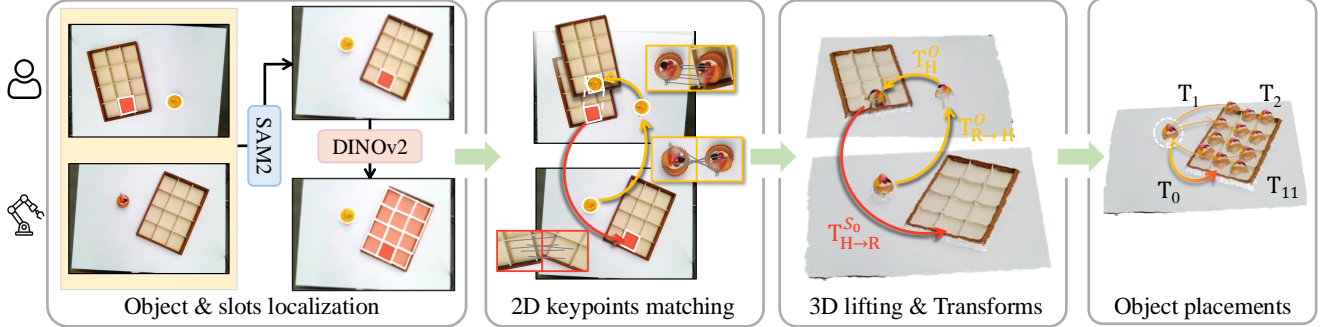


Figure 5. **Correlate with robot view.** Given the object and slot mask detected in the human video, we first re-identify the corresponding object and slot in robot view, and also find all similar empty slots. With corresponding object masks and slot masks, we first compute 2D keypoint matching among the detected object and mask local patches and then lift the observations to 3D to compute 6-DoF transforms.

Object and slot re-identification. Taking as input a short video with only two frames $\{\mathbf{H}_1, \mathbf{R}\}$, SAM2 [54] is employed to output the object mask \mathbf{M}_R^O and one best-matched slot mask $\mathbf{M}_R^{S_0}$ over the robot image \mathbf{R} , given the detected 2D object mask $\mathbf{M}_{H_1}^O$ and the slot mask $\mathbf{M}_{H_1}^S$ on the human first frame image \mathbf{H}_1 . If multiple similar slots are present in the robot image, we leverage SAM [30] to propose segment candidates and use DINOv2 [47] to collect additional slot masks $\{\mathbf{M}_R^{S_1}, \dots, \mathbf{M}_R^{S_k}\}$ that share similar DINOv2 features with the detected slot mask $\mathbf{M}_R^{S_0}$. Empirically, we find that SAM2 and DINOv2 provide good enough performance on our data.

2D keypoint matching. With two corresponding masks in the human view and robot view, we use MAST3R [32] to detect 2D keypoint correspondences by expanding the masks into local 2D bounding boxes. As illustrated in Fig. 5 (middle left), we compute the 2D keypoint matching on two pairs of object local patches (between the object mask \mathbf{M}_R^O in the robot frame and the object mask $\mathbf{M}_{H_1}^O$ in the initial human frame, and between the object mask $\mathbf{M}_{H_n}^O$ in the last human frame and the object mask $\mathbf{M}_{H_1}^O$ in the last human frame) and one pair of slot local patches (between the slot $\mathbf{M}_{H_1}^S$ in the initial human frame and the slot $\mathbf{M}_R^{S_i}$ in the robot view for any slot S_i to place).

3D lifting and transformation calculation. Using the depth sensing and the camera intrinsic parameters, we can lift all human and robot view images into 3D point cloud observations. Then, we are able to lift the 2D keypoint correspondences into 3D correspondences. Equipped with the 3D correspondences, we use Procrustes analysis [20] with RANSAC [18] to calculate three 6-DoF transformation matrices for the aforementioned three local patch pair matchings. We denote the three computed 6-DoF transformations as $T_{R \rightarrow H}^O$, T_H^O , and $T_{H \rightarrow R}^{S_i}$ respectively. Fig. 5 (middle right) illustrates their geometric meanings: the object transformation from the robot scene to the human scene at the start of the human video, the transformation applied by the person to the picked object in the human video, and the slot

transformation from the human scene to the robot scene.

Final object placement transformations. As clearly illustrated in Fig. 5 (middle right and rightmost), by chaining up the three 6-DoF transformation matrix explained above, we can compute the final desired 6-DoF transformation matrix for the robot to execute in order to transform the pick object O from its initial position to any target slot i in the robot coordinate frame as the following

$$\mathbf{T}_i = \mathbf{T}_{H \rightarrow R}^{S_i} \mathbf{T}_H^O \mathbf{T}_{R \rightarrow H}^O. \quad (1)$$

5. Experiments

We propose a new dataset and present an extensive evaluation of our system in Sec. 5.1, where our system, SLeRP, outperforms the baselines by a large margin. In Sec. 5.2, we present an in-depth ablation over Slot-Net and additional design choices in SLeRP. In Sec. 5.3, we show that SLeRP is effective with real-world robots.

5.1. System Evaluation

Given the novelty of the problem we address, existing evaluation benchmarks are unavailable, and there are no baseline methods with which to make direct comparisons. Consequently, we have curated a dataset comprising real-world videos and established a benchmark specific to this problem by developing suitable baselines and metrics.

Dataset. We collected 288 real-world RGB-D videos spanning 9 different object-in-slot task scenarios. For each scenario, variations were introduced in the background and the inclusion of distractor objects, camera positions, and slot occupancy conditions. The suite of tasks includes challenging, common daily activities such as *putting bread into a toaster*, *arranging eggs in an egg steamer*, and *setting mugs on coasters*. All the objects are unseen to Slot-Net during training, and 3 out of the 9 tasks encompass previously unseen task categories. Visualizations of the tasks and their varying settings are provided in the supplementary material.

Benchmark setup. Given that our task necessitates paired data comprising a human demonstration video and a novel

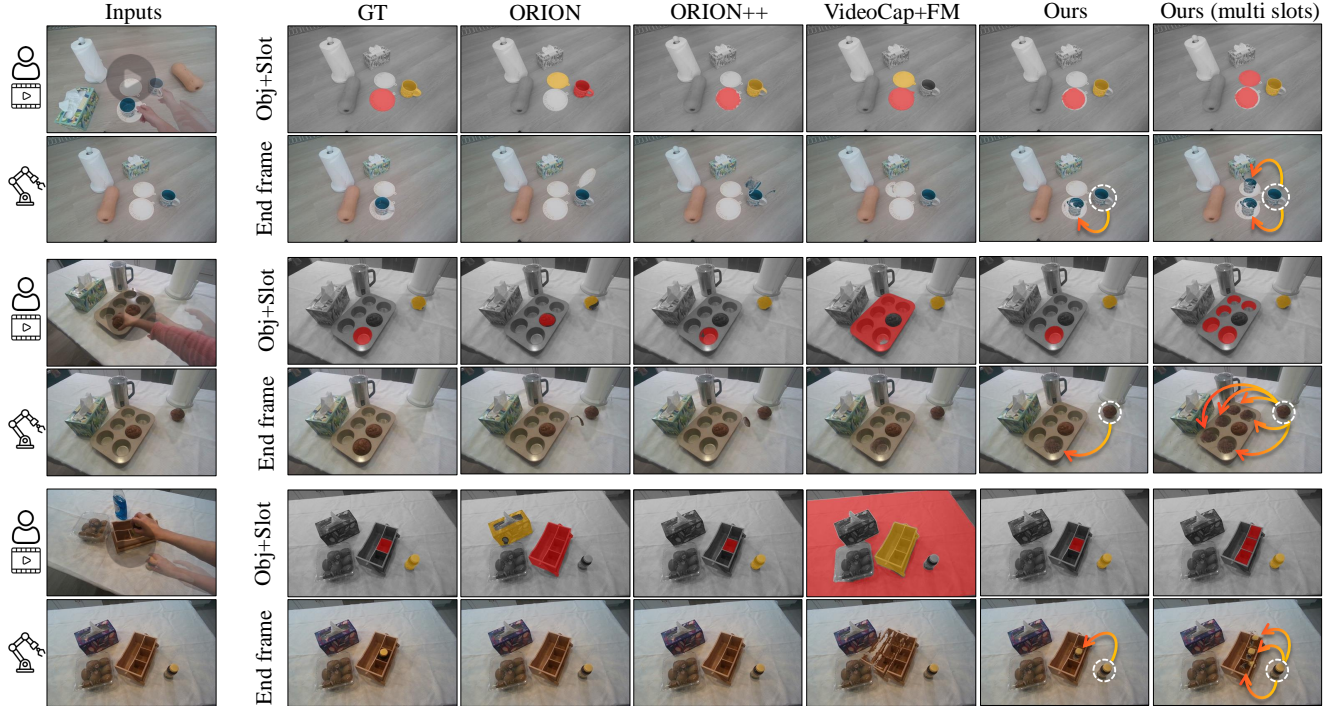


Figure 6. **Qualitative Comparison.** We compare our method to baselines and present side-by-side results on three examples. For each example, the first column shows the input human video at the top and robot-view image in the bottom. The top row displays 2D re-identification results (object in yellow, slot in red), while the bottom row shows 6-DoF relative pose predictions by projecting the object point cloud onto the slots. Unlike the baselines that can only predict one exact slot, our approach can also identify multiple slots. These results clearly demonstrate that our system outperforms the baselines, achieving accurate slot and transformation predictions.

image for the robot’s view, we construct test pairs by repairing the videos in our dataset. Each pair comprises videos depicting the same object being placed into the same slot, albeit with potential variations in background, camera angle, and initial slot occupancy. We designate the first video in each pair as the human demonstration and employ the initial frame of the second video as the robot’s view, as illustrated in Fig. 6. During video data collection, we ensure that human hands are absent in the first frame. We generate three distinct test splits, introducing variations in viewpoint (288 video pairs), background (720 video pairs), and slot occupancy (288 video pairs).

Metrics. We evaluate the accuracy of the predicted 2D masks and the 6-DoF transformation matrix using five distinct metrics. For the evaluation of 2D masks, we calculate (1) the intersection-over-union (IoU) for the object mask and (2) the IoU of the exact slot mask in the robot view, comparing them to their respective ground-truth masks. We assess the accuracy of the 6-DoF transformation by transforming and projecting the object’s point cloud onto the robot view, then measuring (3) the precision of the mask against the ground-truth mask. For 3D evaluation, we compute (4) the Chamfer Distance and (5) Earth Mover’s Distance [16] between the transformed object point cloud and the ground-truth object point cloud at placement. If no mask

or transformation output is predicted for any method, we use a default empty mask and identity matrix as the fallback predictions. To establish ground truths, we annotate the 2D masks of the object and exact slot in the start video frame (*i.e.*, robot’s view), alongside the object’s mask post-placement in the end frame.

Baselines. We design four baselines for comparison.

- *ORION*. Zhu *et al.* [84] perform vision-based human-to-robot imitation learning focused on object-level placement. We adapt ORION to our slot-level setting by providing the required ground-truth object and slot names. In contrast, our method automatically detects in-contact objects and slots without the need of explicit name inputs.
- *ORION++*. We leverage the object and slot detection results from SLeRP to enhance ORION, thereby establishing a stronger baseline.
- *CLIPort++*. CLIPort [60] is an end-to-end imitation-learning-based language-conditioned policy for tabletop tasks. However, the original method requires videos with action labels for training, whereas ours does not. To construct a comparison, we randomly split the tasks into training and test sets, ensuring that tasks, objects, and scenes are unseen during testing, and use the training split to train CLIPort (more details in Supplementary).
- *VideoCap+FM*s. We test whether our proposed tasks

Method	Different view					Different background					Different slot occupancy				
	Obj \uparrow	Slot \uparrow	Prec. \uparrow	CD \downarrow	EMD \downarrow	Obj \uparrow	Slot \uparrow	Prec. \uparrow	CD \downarrow	EMD \downarrow	Obj \uparrow	Slot \uparrow	Prec. \uparrow	CD \downarrow	EMD \downarrow
ORION [84]	0.00	0.11	0.41	0.0949	0.0552	0.45	0.13	0.00	0.0932	0.0540	0.40	0.12	0.82	0.0952	0.0559
ORION++ [84]	10.21	8.89	2.10	0.1058	0.0584	7.53	5.97	0.75	0.1113	0.0597	8.83	7.44	2.95	0.1021	0.0576
CLIPort++ [60]	1.54	0.47	18.75	0.3887	0.1663	1.51	0.35	1.71	0.1152	0.0615	3.06	0.34	12.50	0.1348	0.0681
VideoCap+FM	2.35	8.61	13.45	0.1918	0.0987	2.12	6.28	13.61	0.1743	0.0917	2.64	9.84	7.25	0.1508	0.0837
Ours	73.85	54.37	36.40	0.0282	0.0182	70.27	44.70	25.39	0.0573	0.0323	68.12	47.04	30.30	0.0334	0.0223

Table 1. **Quantitative System Evaluation.** We compare SLeRP with baselines and report the 2D detection and the 3D object transformation accuracy: IoU for the object mask prediction (*Obj*); IoU for the slot mask prediction (*Slot*); mask precision of the predicted object after placement onto the slot projected to the camera plane (*Prec.*); and Chamfer distance (*CD*) and Earth-Mover distance (*EMD*) between the predicted and ground-truth target object point clouds after placement. We evaluate in three different settings with the robot’s views having different camera viewpoints, scene backgrounds, and initial states of the placement slot occupancy compared to the input human videos. We find that SLeRP substantially outperforms the baselines by large margins across all the metrics in all the three evaluation settings.

Method	Synthetic		Real (seen tasks)		Real (unseen tasks)	
	F1 \uparrow	IoU \uparrow	F1 \uparrow	IoU \uparrow	F1 \uparrow	IoU \uparrow
Image difference	44.10	31.34	32.69	20.04	32.20	19.53
Change detection [17]	2.27	1.58	0.06	0.03	6.30	4.19
Object mask	60.16	48.73	65.90	52.10	58.67	42.98
Object-box mask	-	-	43.39	37.74	39.37	34.65
GPT4o+SAM	0.91	0.49	4.82	2.84	4.45	2.68
Slot-Net (end image)	83.44	74.57	48.83	38.68	38.19	28.37
Slot-Net (ours)	82.89	74.62	73.27	61.59	66.50	54.26

Table 2. **Slot Segmentation Results.** We compare Slot-Net against various alternative approaches on slot detection. We evaluate on test synthetic images and our collected real-world images (seen and unseen tasks). Dashes note that the method cannot be evaluated for synthetic data given no video inputs. We can observe clearly that our Slot-Net performs the best.

can be effectively solved using state-of-the-art foundation models. We utilize Qwen2VL [71], a video captioning model, to summarize the video, and then employ GPT4o [2] to identify the object and slot names. Subsequently, we use grounding-SAM2 [55] to generate a bounding box and employ SAM2 [54] to produce the object and slot mask, with the transformation matrix computed using modules in the same way as in our system.

Results. Table 1 presents a quantitative evaluation comparing SLeRP to four baseline methods. The results indicate that SLeRP significantly outperforms all baselines by considerable margins. Fig. 6 offers qualitative comparisons, showcasing 2D object and slot mask predictions alongside 3D object transformation estimations. We observe that SLeRP generates more accurate 2D object and slot detection results, as baseline methods such as ORION and VideoCap+FM frequently struggle to describe slot names in natural language for subsequent visual recognition (e.g., incorrectly detecting the entire placement object or table). Additionally, SLeRP achieves more precise 3D object transformations compared to baselines like CLIPort, which are primarily designed for top-down 2D predictions.

Lastly, our method can fill multiple slots, whereas other methods generate output for only a single slot. In a subset of the data with ground-truth annotations for multiple slots, SLeRP achieves IoU scores of 67.70 and 42.62 for

Method (diff. view)	SlotNet	SAM2	Mast3r	Obj \uparrow	Slot \uparrow	Prec. \uparrow	CD \downarrow	EMD \downarrow
Base design	\times	\times	\times	28.53	28.23	24.72	0.2289	0.1183
Ours w/o SlotNet	\times	\checkmark	\checkmark	73.85	29.63	27.84	0.0486	0.0289
Ours w/o SAM2	\checkmark	\times	\checkmark	31.05	35.98	23.75	0.1219	0.0667
Ours w/o Mast3r	\checkmark	\checkmark	\times	73.85	54.37	32.74	0.0321	0.0205
Ours	\checkmark	\checkmark	\checkmark	73.85	54.37	36.40	0.0282	0.0182

Table 3. **Ablation Study.** All metrics follow Table 1. Results show all the key modules help. See supplementary for the full table.

2D object and slot segmentation. Additionally, it attains scores of 23.14, 0.0575, and 0.0350 for 3D transformation predictions in terms of slot projection precision, Chamfer Distance (CD), and Earth Mover’s Distance (EMD), respectively. These results are comparable to the single-slot placement evaluations reported in Table 1. See the supplementary materials for further details.

5.2. Ablation Study

We evaluate the effectiveness of Slot-Net for placement slot detection in Sec. 5.2.1 and additional ablations on other components like object and slot re-identification and key-point matching in Sec. 5.2.2.

5.2.1. Slot-Net Ablations

Baselines. We consider the following alternative and ablation approaches to replace Slot-Net.

- *Image difference.* We use the difference image between the gray-scale start and end frame, then apply thresholding to the difference image to obtain a mask.
- *Change detection.* We use an off-the-shelf change detection model [17] given two frames for the masks.
- *Object mask.* We directly use the ground-truth pick object mask as the slot mask prediction.
- *Object-box mask.* We take the pick object bounding box detected in the tracking procedure and query SAM for a proxy placement slot mask.
- *GPT4o+SAM.* We query GPT4o with start and end frames for slot bounding boxes and query SAM for masks.
- *Slot-Net (end image).* We use the end frame to replace the difference image as the prompt for Slot-Net.

Benchmark and metrics. We use our newly proposed

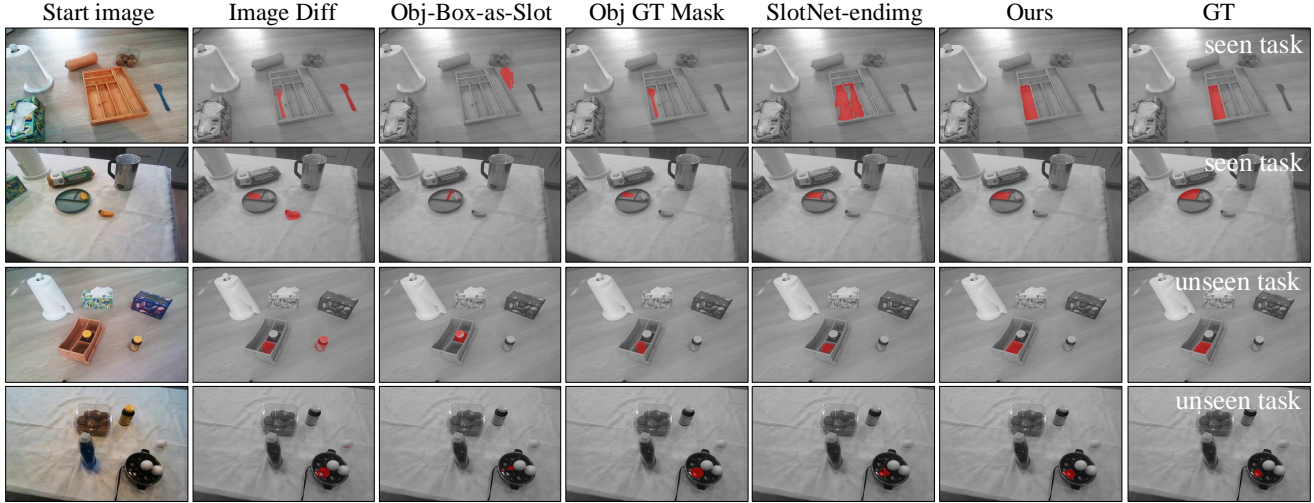


Figure 7. **Slot Detection Comparisons.** We compare Slot-Net to many alternative approaches, and results show that ours performs better.

real-world video dataset along with held-out synthetic images for evaluation. For the real images, we evaluate two splits: *seen tasks*, which involve seen object categories during training but novel object instances, and *unseen tasks*, featuring object categories not encountered during training. For each real-world video, we pair the starting and ending frames as input and evaluate predictions against the ground-truth slot mask from the starting frame. The slot mask prediction performance is assessed using IoU and F1 scores.

Results. Table 2 shows that Slot-Net, when trained on synthetic data, generalizes effectively to real images, outperforming alternative approaches. Fig. 7 provides side-by-side comparisons of different methods, revealing that Slot-Net excels in identifying slot boundaries of various shapes. This underscores the necessity of training a custom model for slot detection and demonstrates that our model is both well-designed and effective.

5.2.2. Other Ablations

Beyond ablating Slot-Net, we further validate two additional key design elements in our system: utilizing SAM2 for object and slot re-identification and employing MAST3R for keypoint matching. In the absence of SAM2, we rely on DINOv2 feature similarity between the slot mask and all SAM-generated masks in the robot image. To replace MAST3R, we employ DINOv2 features for Hungarian matching. Table 3 shows the necessity of these modules.

5.3. Real-Robot Experiments

As shown in Fig. 8, we perform real-robot experiments with a Franka robot and show that SLeRP is effective for real robots. The manipulation system employs a wrist-mounted RGB-D camera (Realsense D415) and an external RGB-D camera (Realsense L515). The camera intrinsics and extrinsics relative to the robot are known. The wrist-mounted camera provides observations for SLeRP, while the exter-

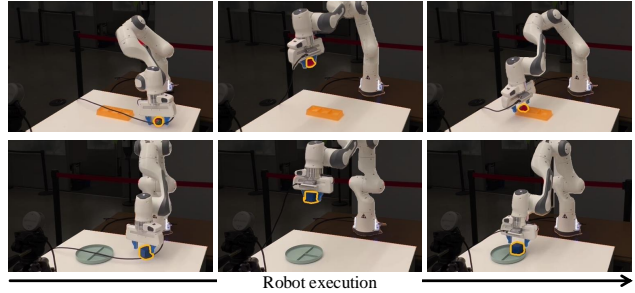


Figure 8. **Real-Robot Experiments.** We show real-robot experiments for “block into a container” and “strawberry into an organizer”. See supplementary for videos and more examples.

nal camera observes the entire scene and aids in planning collision-free trajectories. The system utilizes Contact-Graspnet[67] to generate grasps and plans collision-free trajectories using methods described in [12, 43].

6. Conclusion

In this paper, we address the novel problem of slot-level object placement by learning from a single human demonstration video. We propose a modular system to tackle this problem, which operates without requiring additional training video data and features a unique slot-level placement detector. To evaluate the system’s performance, we introduce a new benchmark consisting of real-world videos and compare our system against key baseline methods. Our results demonstrate that SLeRP outperforms these baselines and functions effectively in real-robot experiments.

Limitations and future work. Given the novel problem formulation, there is potential for further research in fine-grained slot-level object placement with minimal or no human demonstrations. Future work could focus on relaxing current system assumptions, such as the static camera, single-handed interaction, and minimal motion of the placement object. Moreover, advancements in visual foundation

models could enhance the robustness of our system, as they play a crucial role in this work.

References

- [1] Advanced inference: Outpainting. https://huggingface.co/docs/diffusers/en/advanced_inference/outpaint. Accessed: 2010-09-30. 4
- [2] Josh Achiam, Steven Adler, Sandhini Agarwal, Lama Ahmad, Ilge Akkaya, Florencia Leoni Aleman, Diogo Almeida, Janko Altenschmidt, Sam Altman, Shyamal Anadkat, et al. Gpt-4 technical report. *arXiv preprint arXiv:2303.08774*, 2023. 7
- [3] Shikhar Bahl, Abhinav Gupta, and Deepak Pathak. Human-to-robot imitation in the wild. *arXiv preprint arXiv:2207.09450*, 2022. 1, 2
- [4] Shikhar Bahl, Russell Mendonca, Lili Chen, Unnat Jain, and Deepak Pathak. Affordances from human videos as a versatile representation for robotics. In *Proceedings of the IEEE/CVF Conference on Computer Vision and Pattern Recognition*, pages 13778–13790, 2023. 3
- [5] Johannes Baumgartl, Tim Werner, Per Kaminsky, and Dominik Henrich. A fast, gpu-based geometrical placement planner for unknown sensor-modelled objects and placement areas. In *2014 IEEE International Conference on Robotics and Automation (ICRA)*, pages 1552–1559. IEEE, 2014. 2
- [6] Homanga Bharadhwaj, Abhinav Gupta, Vikash Kumar, and Shubham Tulsiani. Towards generalizable zero-shot manipulation via translating human interaction plans. In *2024 IEEE International Conference on Robotics and Automation (ICRA)*, pages 6904–6911. IEEE, 2024. 1, 3
- [7] Homanga Bharadhwaj, Roozbeh Mottaghi, Abhinav Gupta, and Shubham Tulsiani. Track2act: Predicting point tracks from internet videos enables generalizable robot manipulation. In *European Conference on Computer Vision (ECCV)*, 2024. 3
- [8] Anthony Brohan, Noah Brown, Justice Carbajal, Yevgen Chebotar, Joseph Dabis, Chelsea Finn, Keerthana Gopalakrishnan, Karol Hausman, Alex Herzog, Jasmine Hsu, et al. Rt-1: Robotics transformer for real-world control at scale. *arXiv preprint arXiv:2212.06817*, 2022. 1
- [9] Annie S Chen, Suraj Nair, and Chelsea Finn. Learning generalizable robotic reward functions from ”in-the-wild” human videos. *arXiv preprint arXiv:2103.16817*, 2021. 3
- [10] Tianyi Cheng, Dandan Shan, Ayda Sultan Hassen, Richard Ely Locke Higgins, and David Fouhey. Towards a richer 2d understanding of hands at scale. In *Thirty-seventh Conference on Neural Information Processing Systems*, 2023. 4
- [11] Cleanup.pictures. <https://cleanup.pictures>. 4
- [12] Michael Danielczuk, Arsalan Mousavian, Clemens Eppner, and Dieter Fox. Object rearrangement using learned implicit collision functions. In *2021 IEEE International Conference on Robotics and Automation (ICRA)*, pages 6010–6017. IEEE, 2021. 2, 8
- [13] Sudeep Dasari and Abhinav Gupta. Transformers for one-shot visual imitation. In *Conference on Robot Learning*, pages 2071–2084. PMLR, 2021. 3
- [14] Sudeep Dasari, Mohan Kumar Srirama, Unnat Jain, and Abhinav Gupta. An unbiased look at datasets for visuo-motor pre-training. In *Conference on Robot Learning*, pages 1183–1198. PMLR, 2023. 2
- [15] Ben Eisner, Yi Yang, Todor Davchev, Mel Vecerik, Jonathan Scholz, and David Held. Deep se (3)-equivariant geometric reasoning for precise placement tasks. In *The Twelfth International Conference on Learning Representations*. 2
- [16] Haoqiang Fan, Hao Su, and Leonidas J Guibas. A point set generation network for 3d object reconstruction from a single image. In *Proceedings of the IEEE conference on computer vision and pattern recognition*, pages 605–613, 2017. 6
- [17] Sheng Fang, Kaiyu Li, and Zhe Li. Changer: Feature interaction is what you need for change detection. *arXiv preprint arXiv:2209.08290*, 2022. 2, 7
- [18] Martin A Fischler and Robert C Bolles. Random sample consensus: a paradigm for model fitting with applications to image analysis and automated cartography. *Communications of the ACM*, 24(6):381–395, 1981. 5
- [19] Caelan Reed Garrett, Rohan Chitnis, Rachel Holladay, Beomjoon Kim, Tom Silver, Leslie Pack Kaelbling, and Tomás Lozano-Pérez. Integrated task and motion planning. *Annual Review of Control, Robotics, and Autonomous Systems*, 4(1):265–293, 2021. 1
- [20] Colin Goodall. Procrustes methods in the statistical analysis of shape. *Journal of the Royal Statistical Society: Series B (Methodological)*, 53(2):285–321, 1991. 5
- [21] Kensuke Harada, Tokuo Tsuji, Kazuyuki Nagata, Natsuki Yamanobe, and Hiromu Onda. Validating an object placement planner for robotic pick-and-place tasks. *Robotics and Autonomous Systems*, 62(10):1463–1477, 2014. 2
- [22] Joshua A Haustein, Kaiyu Hang, Johannes Stork, and Danica Kragic. Object placement planning and optimization for robot manipulators. In *2019 IEEE/RSJ International Conference on Intelligent Robots and Systems (IROS)*, pages 7417–7424. IEEE, 2019. 2
- [23] Haojie Huang, Dian Wang, Robin Walters, and Robert Platt. Equivariant transporter network. In *Robotics: Science and Systems*, 2022. 2
- [24] Aaron Hurst, Adam Lerer, Adam P Goucher, Adam Perelman, Aditya Ramesh, Aidan Clark, AJ Ostrow, Akila Welihinda, Alan Hayes, Alec Radford, et al. Gpt-4o system card. *arXiv preprint arXiv:2410.21276*, 2024. 2
- [25] Vidhi Jain, Maria Attarian, Nikhil J Joshi, Ayzaan Wahid, Danny Driess, Quan Vuong, Pannag R Sanketi, Pierre Sermanet, Stefan Welker, Christine Chan, et al. Vid2robot: End-to-end video-conditioned policy learning with cross-attention transformers. *arXiv preprint arXiv:2403.12943*, 2024. 1, 3
- [26] Eric Jang, Alex Irpan, Mohi Khansari, Daniel Kappler, Fredrik Ebert, Corey Lynch, Sergey Levine, and Chelsea Finn. Bc-z: Zero-shot task generalization with robotic imitation learning. In *Conference on Robot Learning*, pages 991–1002. PMLR, 2022. 3
- [27] Yun Jiang, Marcus Lim, Changxi Zheng, and Ashutosh Saxena. Learning to place new objects in a scene. *The International Journal of Robotics Research*, 31(9):1021–1043, 2012. 2

- [28] Aditya Kannan, Kenneth Shaw, Shikhar Bahl, Pragna Manam, and Deepak Pathak. Deft: Dexterous fine-tuning for hand policies. In *Conference on Robot Learning*, pages 928–942. PMLR, 2023. 3
- [29] Moo Jin Kim, Karl Pertsch, Siddharth Karamcheti, Ted Xiao, Ashwin Balakrishna, Suraj Nair, Rafael Rafailov, Ethan Foster, Grace Lam, Pannag Sanketi, et al. Openvla: An open-source vision-language-action model. *arXiv preprint arXiv:2406.09246*, 2024. 1
- [30] Alexander Kirillov, Eric Mintun, Nikhila Ravi, Hanzi Mao, Chloe Rolland, Laura Gustafson, Tete Xiao, Spencer Whitehead, Alexander C Berg, Wan-Yen Lo, et al. Segment anything. In *Proceedings of the IEEE/CVF International Conference on Computer Vision*, pages 4015–4026, 2023. 4, 5
- [31] Jangwon Lee and Michael S Ryoo. Learning robot activities from first-person human videos using convolutional future regression. In *Proceedings of the IEEE Conference on Computer Vision and Pattern Recognition Workshops*, pages 1–2, 2017. 2
- [32] Vincent Leroy, Yohann Cabon, and Jérôme Revaud. Grounding image matching in 3d with mast3r. *arXiv preprint arXiv:2406.09756*, 2024. 5
- [33] Siyuan Li, Lei Ke, Martin Danelljan, Luigi Piccinelli, Mattia Segu, Luc Van Gool, and Fisher Yu. Matching anything by segmenting anything. In *Proceedings of the IEEE/CVF Conference on Computer Vision and Pattern Recognition*, pages 18963–18973, 2024. 4
- [34] Weiyu Liu, Chris Paxton, Tucker Hermans, and Dieter Fox. Structformer: Learning spatial structure for language-guided semantic rearrangement of novel objects. In *2022 International Conference on Robotics and Automation (ICRA)*, pages 6322–6329. IEEE, 2022. 2
- [35] YuXuan Liu, Abhishek Gupta, Pieter Abbeel, and Sergey Levine. Imitation from observation: Learning to imitate behaviors from raw video via context translation. In *2018 IEEE international conference on robotics and automation (ICRA)*, pages 1118–1125. IEEE, 2018. 3
- [36] Tomás Lozano-Pérez, Joseph L. Jones, Emmanuel Mazer, and Patrick A. O’Donnell. Task-level planning of pick-and-place robot motions. *Computer*, 22(3):21–29, 1989. 2
- [37] Yecheng Jason Ma, Shagun Sodhani, Dinesh Jayaraman, Osbert Bastani, Vikash Kumar, and Amy Zhang. Vip: Towards universal visual reward and representation via value-implicit pre-training. In *The Eleventh International Conference on Learning Representations*. 3
- [38] Arjun Majumdar, Karmesh Yadav, Sergio Arnaud, Jason Ma, Claire Chen, Sneha Silwal, Aryan Jain, Vincent-Pierre Berges, Tingfan Wu, Jay Vakil, et al. Where are we in the search for an artificial visual cortex for embodied intelligence? *Advances in Neural Information Processing Systems*, 36:655–677, 2023. 2
- [39] Zhao Mandi, Fangchen Liu, Kimin Lee, and Pieter Abbeel. Towards more generalizable one-shot visual imitation learning. In *2022 International Conference on Robotics and Automation (ICRA)*, pages 2434–2444. IEEE, 2022. 3
- [40] Priyanka Mandikal and Kristen Grauman. Dexvip: Learning dexterous grasping with human hand pose priors from video. In *Conference on Robot Learning*, pages 651–661. PMLR, 2022. 3
- [41] Oier Mees, Alp Emek, Johan Vertens, and Wolfram Burgard. Learning object placements for relational instructions by hallucinating scene representations. In *2020 IEEE International Conference on Robotics and Automation (ICRA)*, pages 94–100. IEEE, 2020. 2
- [42] Chaitanya Mitash, Rahul Shome, Bowen Wen, Abdeslam Boularias, and Kostas Bekris. Task-driven perception and manipulation for constrained placement of unknown objects. *IEEE Robotics and Automation Letters*, 5(4):5605–5612, 2020. 2
- [43] Adithyavairavan Murali, Arsalan Mousavian, Clemens Eppner, Adam Fishman, and Dieter Fox. Cabinet: Scaling neural collision detection for object rearrangement with procedural scene generation. In *2023 IEEE International Conference on Robotics and Automation (ICRA)*, pages 1866–1874. IEEE, 2023. 2, 8
- [44] Suraj Nair, Aravind Rajeswaran, Vikash Kumar, Chelsea Finn, and Abhinav Gupta. R3m: A universal visual representation for robot manipulation. In *Conference on Robot Learning*, pages 892–909. PMLR, 2023. 2
- [45] Rhys Newbury, Kerry He, Akansel Cosgun, and Tom Drummond. Learning to place objects onto flat surfaces in upright orientations. *IEEE Robotics and Automation Letters*, 6(3):4377–4384, 2021. 2
- [46] Anh Nguyen, Dimitrios Kanoulas, Luca Muratore, Darwin G Caldwell, and Nikos G Tsagarakis. Translating videos to commands for robotic manipulation with deep recurrent neural networks. In *2018 IEEE International Conference on Robotics and Automation (ICRA)*, pages 3782–3788. IEEE, 2018. 2
- [47] Maxime Oquab, Timothée Darcet, Théo Moutakanni, Huy V Vo, Marc Szafraniec, Vasil Khalidov, Pierre Fernandez, Daniel HAZIZA, Francisco Massa, Alaaeldin El-Nouby, et al. Dinov2: Learning robust visual features without supervision. *Transactions on Machine Learning Research*. 5
- [48] Helena Örnkloo and Claes von Hofsten. Fitting objects into holes: on the development of spatial cognition skills. *Developmental psychology*, 43(2):404, 2007. 1
- [49] Chuer Pan, Brian Okorn, Harry Zhang, Ben Eisner, and David Held. Tax-pose: Task-specific cross-pose estimation for robot manipulation. In *Conference on Robot Learning*, pages 1783–1792. PMLR, 2023. 2
- [50] Austin Patel, Andrew Wang, Ilija Radosavovic, and Jitendra Malik. Learning to imitate object interactions from internet videos. *arXiv:2211.13225*, 2022. 3
- [51] Chris Paxton, Chris Xie, Tucker Hermans, and Dieter Fox. Predicting stable configurations for semantic placement of novel objects. In *5th Annual Conference on Robot Learning*. 2
- [52] Dustin Podell, Zion English, Kyle Lacey, Andreas Blattmann, Tim Dockhorn, Jonas Müller, Joe Penna, and Robin Rombach. Sdxl: Improving latent diffusion models for high-resolution image synthesis. In *The Twelfth International Conference on Learning Representations*. 4
- [53] Yuzhe Qin, Yueh-Hua Wu, Shaowei Liu, Hanwen Jiang, Ruihan Yang, Yang Fu, and Xiaolong Wang. Dexmv: Imitation

- learning for dexterous manipulation from human videos. In *European Conference on Computer Vision*, pages 570–587. Springer, 2022. 3
- [54] Nikhila Ravi, Valentin Gabeur, Yuan-Ting Hu, Ronghang Hu, Chaitanya Ryali, Tengyu Ma, Haitham Khedr, Roman Rädle, Chloe Rolland, Laura Gustafson, et al. Sam 2: Segment anything in images and videos. *arXiv preprint arXiv:2408.00714*, 2024. 4, 5, 7
- [55] Tianhe Ren, Qing Jiang, Shilong Liu, Zhaoyang Zeng, Wenlong Liu, Han Gao, Hongjie Huang, Zhengyu Ma, Xiaoke Jiang, Yihao Chen, Yuda Xiong, Hao Zhang, Feng Li, Peijun Tang, Kent Yu, and Lei Zhang. Grounding dino 1.5: Advance the "edge" of open-set object detection, 2024. 7
- [56] Brian Rooks. Machine tending in the modern age. *Industrial Robot: An International Journal*, 30(4):313–318, 2003. 1
- [57] Jinghuan Shang, Karl Schmeckpeper, Brandon B May, Maria Vittoria Minniti, Tarik Kelestemur, David Watkins, and Laura Herlant. Theia: Distilling diverse vision foundation models for robot learning. In *8th Annual Conference on Robot Learning*. 2
- [58] Aditya Sharma, Luke Yoffe, and Tobias Höllerer. Octo+: A suite for automatic open-vocabulary object placement in mixed reality. In *2024 IEEE International Conference on Artificial Intelligence and eXtended and Virtual Reality (AIxVR)*, pages 157–165. IEEE, 2024. 2
- [59] Kenneth Shaw, Shikhar Bahl, and Deepak Pathak. Videodex: Learning dexterity from internet videos. In *Conference on Robot Learning*, pages 654–665. PMLR, 2023. 3
- [60] Mohit Shridhar, Lucas Manuelli, and Dieter Fox. Cliport: What and where pathways for robotic manipulation. In *Proceedings of the 5th Conference on Robot Learning (CoRL)*, 2021. 2, 6, 7
- [61] Anthony Simeonov, Yilun Du, Andrea Tagliasacchi, Joshua B Tenenbaum, Alberto Rodriguez, Pulkit Agrawal, and Vincent Sitzmann. Neural descriptor fields: Se (3)-equivariant object representations for manipulation. In *2022 International Conference on Robotics and Automation (ICRA)*, pages 6394–6400. IEEE, 2022. 2
- [62] Anthony Simeonov, Yilun Du, Yen-Chen Lin, Alberto Rodriguez Garcia, Leslie Pack Kaelbling, Tomás Lozano-Pérez, and Pulkit Agrawal. Se (3)-equivariant relational rearrangement with neural descriptor fields. In *Conference on Robot Learning*, pages 835–846. PMLR, 2023. 2
- [63] Himanshu Gaurav Singh, Antonio Loquercio, Carmelo Sferazza, Jane Wu, Haozhi Qi, Pieter Abbeel, and Jitendra Malik. Hand-object interaction pretraining from videos. *arXiv preprint arXiv:2409.08273*, 2024. 3
- [64] Toronto Annotation Suite. <https://aidemos.cs.toronto.edu/toras>. 4
- [65] Yu Sun, Shaogang Ren, and Yun Lin. Object-object interaction affordance learning. *Robotics and Autonomous Systems*, 62(4):487–496, 2014. 2
- [66] Balakumar Sundaralingam, Siva Kumar Sastry Hari, Adam Fishman, Caelan Garrett, Karl Van Wyk, Valts Blukis, Alexander Millane, Helen Millane, Ankur Handa, Fabio Ramos, Nathan Ratliff, and Dieter Fox. CuRobo: Parallelized collision-free robot motion generation. In *ICRA*, 2023. 1
- [67] Martin Sundermeyer, Arsalan Mousavian, Rudolph Triebel, and Fox Dieter. Contact-graspnet: Efficient 6-dof grasp generation in cluttered scenes. *IEEE International Conference on Robotics and Automation (ICRA)*, 2021. 8
- [68] Hugo Touvron, Thibaut Lavril, Gautier Izacard, Xavier Martinet, Marie-Anne Lachaux, Timothée Lacroix, Baptiste Rozière, Naman Goyal, Eric Hambro, Faisal Azhar, et al. Llama: Open and efficient foundation language models. *arXiv preprint arXiv:2302.13971*, 2023. 4
- [69] Patrick von Platen, Suraj Patil, Anton Lozhkov, Pedro Cuenca, Nathan Lambert, Kashif Rasul, Mishig Davaadorj, Dhruv Nair, Sayak Paul, William Berman, Yiyi Xu, Steven Liu, and Thomas Wolf. Diffusers: State-of-the-art diffusion models. <https://github.com/huggingface/diffusers>, 2022. 4
- [70] Chen Wang, Linxi Fan, Jiankai Sun, Ruohan Zhang, Li Fei-Fei, Danfei Xu, Yuke Zhu, and Anima Anandkumar. Mimicplay: Long-horizon imitation learning by watching human play. *arXiv preprint arXiv:2302.12422*, 2023. 2
- [71] Peng Wang, Shuai Bai, Sinan Tan, Shijie Wang, Zhihao Fan, Jinze Bai, Keqin Chen, Xuejing Liu, Jialin Wang, Wenbin Ge, Yang Fan, Kai Dang, Mengfei Du, Xuancheng Ren, Rui Men, Dayiheng Liu, Chang Zhou, Jingren Zhou, and Junyang Lin. Qwen2-vl: Enhancing vision-language model's perception of the world at any resolution. *arXiv preprint arXiv:2409.12191*, 2024. 7
- [72] Yixuan Wang, Mingtong Zhang, Zhuoran Li, Tarik Kelestemur, Katherine Rose Driggs-Campbell, Jiajun Wu, Li Fei-Fei, and Yunzhu Li. D3 fields: Dynamic 3d descriptor fields for zero-shot generalizable rearrangement. In *8th Annual Conference on Robot Learning*, 2024. 2
- [73] Chuan Wen, Xingyu Lin, John So, Kai Chen, Qi Dou, Yang Gao, and Pieter Abbeel. Any-point trajectory modeling for policy learning. In *Robotics: Science and Systems*, 2024. 3
- [74] Hongtao Wu, Jikai Ye, Xin Meng, Chris Paxton, and Gregory S Chirikjian. Transporters with visual foresight for solving unseen rearrangement tasks. In *2022 IEEE/RSJ International Conference on Intelligent Robots and Systems (IROS)*, pages 10756–10763. IEEE, 2022. 2
- [75] Haoyu Xiong, Quanzhou Li, Yun-Chun Chen, Homanga Bharadhwaj, Samarth Sinha, and Animesh Garg. Learning by watching: Physical imitation of manipulation skills from human videos. In *2021 IEEE/RSJ International Conference on Intelligent Robots and Systems (IROS)*, pages 7827–7834. IEEE, 2021. 1, 3
- [76] Mengda Xu, Zhenjia Xu, Yinghao Xu, Cheng Chi, Gordon Wetzstein, Manuela Veloso, and Shuran Song. Flow as the cross-domain manipulation interface. In *8th Annual Conference on Robot Learning*. 3
- [77] Yezhou Yang, Yi Li, Cornelia Fermuller, and Yiannis Aloimonos. Robot learning manipulation action plans by "watching" unconstrained videos from the world wide web. In *Proceedings of the AAAI conference on artificial intelligence*, 2015. 3
- [78] Seonghyeon Ye, Joel Jang, Byeongguk Jeon, SeJune Joo, Jianwei Yang, Baolin Peng, Ajay Mandlikar, Reuben Tan, Yu-Wei Chao, Bill Yuchen Lin, et al. Latent action pretraining from videos. *arXiv preprint arXiv:2410.11758*, 2024. 2

- [79] Tianhe Yu, Chelsea Finn, Sudeep Dasari, Annie Xie, Tianhao Zhang, Pieter Abbeel, and Sergey Levine. One-shot imitation from observing humans via domain-adaptive meta-learning. *Robotics: Science and Systems XIV*, 2018. [3](#)
- [80] Chengbo Yuan, Chuan Wen, Tong Zhang, and Yang Gao. General flow as foundation affordance for scalable robot learning. *arXiv preprint arXiv:2401.11439*, 2024. [3](#)
- [81] Wentao Yuan, Adithyavairavan Murali, Arsalan Mousavian, and Dieter Fox. M2t2: Multi-task masked transformer for object-centric pick and place. In *7th Annual Conference on Robot Learning*. [2](#)
- [82] Kevin Zakka, Andy Zeng, Johnny Lee, and Shuran Song. Form2fit: Learning shape priors for generalizable assembly from disassembly. In *2020 IEEE International Conference on Robotics and Automation (ICRA)*, pages 9404–9410. IEEE, 2020. [2](#)
- [83] Andy Zeng, Pete Florence, Jonathan Tompson, Stefan Welker, Jonathan Chien, Maria Attarian, Travis Armstrong, Ivan Krasin, Dan Duong, Vikas Sindhwani, et al. Transporter networks: Rearranging the visual world for robotic manipulation. In *Conference on Robot Learning*, pages 726–747. PMLR, 2021. [2](#)
- [84] Yifeng Zhu, Arisrei Lim, Peter Stone, and Yuke Zhu. Vision-based manipulation from single human video with open-world object graphs. *arXiv preprint arXiv:2405.20321*, 2024. [1](#), [2](#), [3](#), [6](#), [7](#)